Decolorization of Azo Dyes in Bioelectrochemical Systems

ARTICLE *in* ENVIRONMENTAL SCIENCE AND TECHNOLOGY · AUGUST 2009

Impact Factor: 5.33 · DOI: 10.1021/es900057f · Source: PubMed

Environ. Sci. Technol. **2009,** *43,* 5137–5143

Decolorization of Azo Dyes in Bioelectrochemical Systems

YANG MU,* KORNEEL RABAEY, RENÉ A. ROZENDAL, ZHIGUO YUAN, AND JÜRG KELLER

Advanced Water Management Centre, The University of Queensland, St. Lucia, QLD 4072, Australia

Received January 8, 2009. Revised manuscript received May 5, 2009. Accepted May 11, 2009.

Azo dyes are ubiquitously used in the textile industry. These dyes need to be removed from the effluent prior to discharge to sewage due to their intense color and toxicity. In this study we investigated the use of a bioelectrochemical system (BES) to abioticlly cathodic decolorization of a model azo dye, Acid Orange 7 (AO7), where the process was driven by microbial oxidation of acetate at the anode. Effective decolorization of AO7 at rates up to 2.64 ± 0.03 mol m^{-3} NCC d^{-1} (net cathodic compartment, NCC) was achieved at the cathode, with concomitant energy recovery. The AO7 decolorization rate was significantly enhanced when the BES was supplied with power, reaching 13.18 ± 0.05 mol m^{-3} NCC d^{-1} at an energy consumption 0.012 ± 0.001 kWh mol^{-1} AO7 (at a controlled cathode potential of −400 mV vs SHE). Compared with conventional anaerobic biological methods, the required dosage of organic cosubstrate was significantly reduced in the BES. A possible cathodic reaction mechanism for the decolorization of AO7 is suggested based on the decolorization products identified: the azo bond of AO7 was cleaved at the cathode, resulting in the formation of the colorless sulfanilic acid and 1-amino-2-naphthol.

Introduction

Azo dyes are the largest and most versatile class of dyes and are widely used in the textile, leather, plastics, cosmetics, and food industry (*1*). They are characterized by containing one or more azo groups (—N═N—), with most of them being xenobiotics. They end up in industrial wastewaters—and potentially in the environment—due to the fact that not all dye molecules bind to the fabric during the dyeing process. Depending on the dye class, between 2% and as much as 50% of the dye used ends up in the wastewater (*2*). This discharge is undesirable, not only because of their color but also because many azo dyes and their breakdown products are toxic and/or mutagenic (*3*).

A range of physicochemical methods exists to remove color from dye containing effluents (*4, 5*). Extensively used are coagulation/flocculation processes. They require significant quantities of chemicals and produce notable amounts of sludge, requiring further handling and disposal. Adsorption and membrane filtration techniques lead to secondary waste streams which need further treatment and/or disposal. Both advanced oxidation processes (AOPs, such as ozonation, UV/H_2O_2, Fenton, etc.) and membrane filtration methods can be quite effective for color removal but are energy and cost intensive (*6*). Few studies have reported electrochemical decolorization of azo dyes at the cathode from wastewater (*7, 8*). In these reported studies, oxygen was produced from H_2O at the anode and the azo dye was simultaneously reduced using protons and electrons at the cathode. Such a process has potential advantages in terms of versatility, environmental compatibility, and no chemical usage. However, chemical catalysts were used in both anodes and cathodes in these studies, resulting in high overpotentials at both electrodes and accordingly high energy consumption. For instance, the cathodic decolorization of textile wastewater containing azo dye CI acid red 27 was achieved at laboratory scale with an energy consumption of about 11.2 kWh mol^{-1} azo dye (*7*).

Azo dyes are generally persistent under aerobic conditions (*9*). Biological decolorization via anaerobic reductive processes presents a less expensive alternative but is usually very slow and requires an electron donor (organic cosubstrate) to create the necessary reductive conditions (*10*). The cosubstrate addition typically far exceeds the stoichiometric requirements, leading to additional costs and unwanted methane production (*11*).

In recent years, microbial fuel cells (MFCs) and microbial electrolysis cells (MECs) have been explored extensively for their innovative features and environmental benefits (*12, 13*). At the anode, organic material from the wastewater is oxidized by electrochemically active microorganisms. Subsequently, the microorganisms transfer the electrons resulting from this oxidation to the anode via extracellular electron transfer. Through an electrical circuit, the electrons are transported to the cathode, where they are consumed for oxygen reduction (in the case of MFCs) or hydrogen formation (in the case of MECs). Both cathodic reactions can occur either through direct chemical catalysis (e.g., with platinum) or through biocatalysis (in the case of a microbial biocathode). In an MFC, electrical energy can be extracted from the electrical circuit. In an MEC, however, electrical energy needs to be supplied to the electrical circuit by means of a power supply.

Since energy generation is not always the aim of this technology, a more appropriate term, bioelectrochemical system (BES), has been recently introduced (*14*). A number of valuable oxidation or reduction reactions demonstrating the versatility of BESs have been described. For example, BES systems have been applied to remove organic and inorganic contaminants such as acetate (*15*), cellulose (*16*), rhizodeposits of rice plants (*17*), and sulfur (*18*) from wastewater at the anode chamber. On the other hand, BESs can reduce nitrate and nitrite (*19, 20*), and reductively dehalogenate (*21*) at the cathode.

The present study aims to investigate whether azo dyes can be reduced at the abiotic cathode of a BES, where the process is driven by microbial oxidation of organics at the anode. The standard electron potentials for the reduction of azo dyes to their constituent aromatic amines are not available and reported half-cell potentials range between −530 and −180 mV vs SHE (*22*). Acid Orange 7 (AO7) was used as a model compound since it is a well-known azo dye that is widely used in the textile, food, and cosmetics industries, thus appearing in these manufacturing wastewaters. Our hypothesis is that one N═N double bond in the AO7 structure can be broken completely after accepting four electrons from the cathode, resulting in the formation of colorless sulfanilic acid and 1-amino-2-naphthol. The focus of this study was on the feasibility of the process and electron balance, as well as the identification of the breakdown products.

* Corresponding author phone: +61 7 3346 7211; fax: +61 7 3365 4726; e-mail: yangmu@awmc.uq.edu.au.

10.1021/es900057f CCC: $40.75
Published on Web 05/27/2009

Materials and Methods

Chemicals. Sodium acetate, Acid Orange 7, sulfanilic acid, and 1-amino-2-naphthol were obtained from Sigma-Aldrich (Sydney, Australia). Sulfanilic acid and 1-amino-2-naphthol were used for the byproduct identification and quantification using the HPLC method.

Bioelectrochemical System. The BES was constructed by assembling two equal rectangular Perspex frames with internal dimensions of $0.14 \times 0.12 \times 0.2$ m^3. The frames were bolted together between two Perspex square plates. A cation exchange membrane (Ultrex CMI-7000, Membranes International, U.S.) was placed between the anode and the cathode as illustrated in Freguia et al. (*23*). Sealing was ensured by rubber sheets inserted between each frame. The total empty volume for each compartment was 336×10^{-6} m^3 (Total cathodic compartment, TCC). Granular graphite with diameter ranging from 2 to 6 mm (El Carb 100, Graphite Sales, Inc., U.S.) was used as electrode in both the anode and cathode compartments, reducing the compartment liquid volume to 182×10^{-6} m^3 (net cathodic compartment, NCC; net anodic compartment, NAC). Prior to use, the granular graphite was washed for 24 h in 32% HCl four times, in order to eliminate any potentially catalytic foreign compounds from the graphite material (*23*). A graphite rod (5 mm diameter) was used in both the anodic and cathodic compartments to connect the electrodes to the external circuit. By killing all microorganisms, this treatment also eliminated any potential biocatalyst that could have affected the cathode performance. To ensure that biological activity would not influence the results, the experiments were started immediately after adding the pretreated granules to the reactor. The fact that the cathode performance was established very quickly and did not change over time strongly indicates that no biocatalysis was developing during the operation of this reactor.

During the startup, the anodic compartment of the BES was inoculated with a microbial consortium previously enriched in MFCs with acetate as the carbon source, and continuously fed with a modified M9 medium as described previously (*24*). The growth medium with 320 mg/L sodium acetate as electron donor was fed to the anodic reactor at a flow rate of 540×10^{-6} m^3 d^{-1}, giving rise to an organic loading rate of 0.8 kg COD m^{-3} NAC d^{-1}. The influent catholyte of BES only included a 50 mM phosphate buffer (17.2 mM KH_2PO_4 and 32.8 mM Na_2HPO_4) and the model azo dye AO7 with the concentration 0.19 mM. The influents of both the anode and the cathode were sparged with nitrogen gas for 10 min after their preparation to remove possible dissolved oxygen from the solutions. The hydraulic retention time (HRT) in the cathode was 1.44 h and the external resistance of BES was 8.5 Ω during the startup period. After 6 weeks of operation, the anode potential at open circuit reached −330 mV vs SHE, indicating the successful startup of the BES reactor.

Open circuit experiments with continuous cathode feeding mode were conducted initially at various AO7 concentrations while keeping other parameters (flow rate, pH) unchanged and each experiment lasted 1−2 weeks. The purpose of these control experiments was to confirm that the removal of AO7 was not due to adsorption onto the graphite granules or associated with the catalytic activity of the graphite material. Then the circuit of the BES was closed again and a series of experiments were conducted in order to investigate the influence of various operational parameters on AO7 decolorization. The variations in the operational parameters are listed in Supporting Information (SI) Table S1. The pH of the influent AO7 solution was maintained at 7.0 using 50 mM phosphate buffer (17.2 mM KH_2PO_4 and 32.8 mM Na_2HPO_4) in all experiments, except for pH 5.5 and 9.4 in series 3. To maintain a pH of 5.5 in the influent AO7 solution, a buffer with 48 mM KH_2PO_4 and 2 mM Na_2HPO_4 was used, whereas a pH of 9.4 was achieved using 50 mM Na_2HPO_4. After these, one additional experiment was carried out without phosphate buffer in the influent AO7 solution, whereas the pH was adjusted to 7 using 0.1 mM HCl. Each experiment lasted 1−2 weeks to ensure that the reactor reached steady-state, judging from the constant AO7 decolorization efficiency and rate, and the constant anode and cathode potentials. Only those results obtained under steady-state conditions are reported in this paper.

Throughout the experiments, both anolyte and catholyte were recirculated at a rate of approximately 200 mL min^{-1} to maintain well-mixed conditions and to avoid concentration gradients and clogging of the granular matrix during continuous feed. The recirculation tubing was made of low gas-permeable PVC material and was kept as short as possible to minimize introduction of O_2. The cathodic half-cell potentials were measured by placing an Ag/AgCl reference electrode (assumed +0.197 V vs SHE) (ref 201, BioAnalytical Systems) in the cathode compartment of each BES. All experiments were performed at 25 ± 1 °C.

Chemical Analysis. Throughout the experiments, samples taken from the cathode were immediately filtered through a 0.22 μm filter, and AO7 concentrations were measured using UV−vis spectrophotometer (Cary 50, Varian Inc.) at 484 nm. The UV−vis absorption spectra of AO7 and the decolorized samples were recorded over a wavelength range from 200 to 800 nm using UV−vis spectrophotometry. The reduced products of the AO7 decolorization were identified and quantified using high performance liquid chromatography (HPLC). The HPLC system (model-600, Waters Co.) used a Phenomenex Gemini C18 column (5 μm; 150 × 4.6 mm) for separation and a UV detector (model-2487, Waters Co.) for measurement at 254 nm. The mobile phase (50% methanol, 50% 33 mM phosphate buffer at pH 7.0) was pumped at a rate of 1.0 mL min^{-1}.

The AO7 decolorization efficiency (DE) and rate (DR: mol m^{-3} NCC d^{-1}) were calculated as follows:

$$\mathrm{DE} = \frac{C_{\text{in-AO7}} - C_{\text{ef-AO7}}}{C_{\text{in-AO7}}} \times 100(\%) \quad (1)$$

$$\mathrm{DR} = \frac{(C_{\text{in-AO7}} - C_{\text{ef-AO7}}) \times Q_{\mathrm{C}}}{\mathrm{NCC}} \quad (2)$$

where $C_{\text{in−AO7}}$ is the influent AO7 concentration (mM), $C_{\text{ef−AO7}}$ is the effluent AO7 concentration (mM), and Q_{C} is the influent flow rate of the cathode (m^3 d^{-1}).

In order to calculate the Coulombic efficiency on acetate oxidation at the anode in Series 1, the samples from the anode effluent were immediately filtered through a 0.22 μm filter and the acetate concentrations were determined. For acetate analysis, a 0.9 mL sample was added to 0.1 mL of 10% formic acid solution and analyzed with a gas chromatography method using a polar capillary column (DB-FFAP) at 140 °C and a flame ionization detector at 250 °C.

Electrochemical Monitoring and Calculation. The graphite rod contacts of both the anodic and the cathodic electrode were connected to an external resistance or to a potentiostat (VMP3 multichannel potentiostat, Princeton Applied Research, U.S.) for cathodic potential control. Calculations were performed according to Logan et al. (*12*).

The current was calculated from the external resistance using Ohm's law. The Coulombic efficiency for acetate oxidation ($\varepsilon_{\mathrm{Ac}}$) was evaluated according to Logan et al. (*12*):

$$\varepsilon_{\mathrm{Ac}} = \frac{I}{4 \times \Delta\mathrm{COD} \times \dfrac{Q_{\mathrm{A}} \times 10^3}{24 \times 3600} \times F} \quad (3)$$

where I is the current (mA), F is Faraday's constant (96485 C mol^{-1} e), ΔCOD is the change of acetate concentration in COD (mM), 4 is the number of electrons exchanged per mole of COD, Q_A is the influent flow rate of anode (m^3 d^{-1}).

The Coulombic efficiency for AO7 decolorization (ε_{AO7}) was calculated as the ratio of the theoretical current estimation based on the full azo bond reduction of AO7 at the cathode and the current flowing across the BESs:

$$\varepsilon_{AO7} = \frac{4 \times (C_{in\text{-}AO7} - C_{ef\text{-}AO7}) \times \dfrac{Q_C \times 10^3}{24 \times 3600} \times F}{I} \quad (4)$$

where 4 is the number moles of electrons that can be accepted by 1 mol of AO7 in the cathodic compartment assuming the complete breakdown of the azo bond. The Coulombic efficiency for SA formation (ε_{SA}) was calculated as the ratio of the theoretical current estimation based on the SA production from AO7 at the cathode and the current flowing across the BES:

$$\varepsilon_{SA} = \frac{4 \times C_{ef\text{-}SA} \times \dfrac{Q_C \times 10^3}{24 \times 3600} \times F}{I} \quad (5)$$

where 4 is the number moles of electrons when SA formed from AO7, $C_{ef\text{-}SA}$ is the effluent SA concentration (mM).

As with conventional anaerobic biological methods, an electron donor (organic cosubstrate or reductant) such as acetate is required at the anode of BES to supply electrons for the AO7 reduction at the cathode. In order to compare the dosage of the electron donor, the reductant usage ratio (RUR) was defined as the moles of COD consumption per mol AO7 removal (mol COD mol^{-1} AO7) in the reactors. It can be calculated in the BES as follows:

$$RUR = \frac{\Delta COD \times Q_A}{(C_{in\text{-}AO7} - C_{ef\text{-}AO7}) \times Q_C} \quad (6)$$

Substituting eqs 3 and 4 into eq 6 this becomes

$$RUR = \frac{6 \times 3600 \times I}{\varepsilon_{Ac} \times F} \times \frac{F}{I \times \varepsilon_{AO7} \times 3600 \times 6} = \frac{1}{\varepsilon_{Ac}} \times \frac{1}{\varepsilon_{AO7}} \quad (7)$$

Results and Discussion

Simultaneous AO7 Decolorization and Electricity Generation. During the continuous cathode feeding, the adsorption effect of AO7 onto the cathode granules can be excluded once steady state performance is achieved as the adsorption would have reached saturation state. As illustrated in Figure 1(A), both the AO7 decolorization efficiency and rate were very small under open circuit conditions, which also indicates that nonelectrochemical reactions at the graphite electrode surface were minimal, resulting in a minor effect on AO7 decolorization. During closed circuit operation (at 8.5 Ω external resistance), both the decolorization efficiency and rate of AO7 were significantly enhanced, demonstrating that the cathode was used as the electron donor for AO7 decolorization. As the influent AO7 concentration increased from 0.19 to 0.70 mM, the AO7 decolorization efficiency was decreased from 78.7 ± 0.7% to 35.0 ± 2.0%. However, the AO7 decolorization rate increased at the same time from 2.48 ± 0.02 to 4.08 ± 0.24 mol m^{-3} NCC d^{-1}. Power was also generated simultaneously with the AO7 decolorization, as shown in Figure 1(B). The current density increased from 14.2 ± 1.0 to 19.7 ± 0.9 A m^{-3} NCC and the power output increased from 0.31 ± 0.03 to 0.60 ± 0.02 W m^{-3} NCC, as the influent AO7 concentration increased from 0.19 to 0.70 mM.

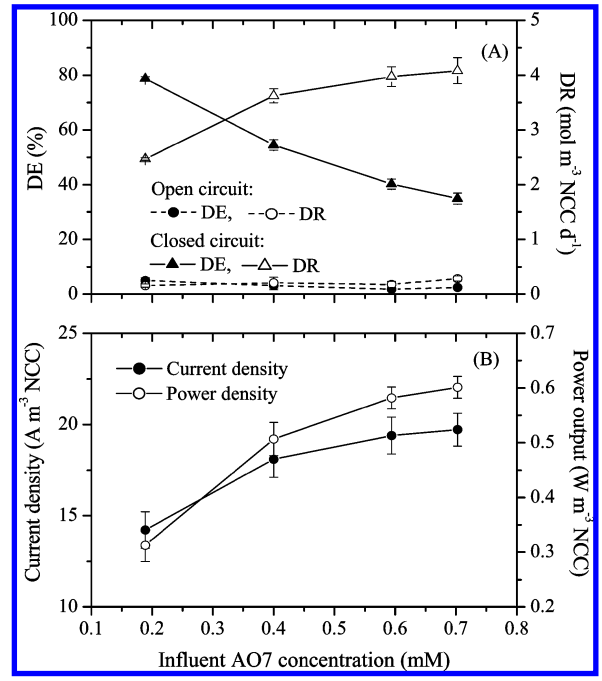

FIGURE 1. Effect of influent AO7 concentration on (A) decolorization efficiency (DE) and rate (DR) at open circuit and closed circuit, (B) Current and power generation at closed circuit in BES (HRT 1.44 h, external resistance 8.5 Ω, pH 7.0).

The AO7 decolorization activity in BES was also monitored at different external resistances, as shown in SI Figure S1(A). When the external resistance was increased from 3.2 to 100 Ω, the AO7 decolorization efficiency decreased from 83.1 ± 0.5% to 3.5 ± 0.8%, and the decolorization rate decreased from 2.63 ± 0.02 to 0.11 ± 0.03 mol m^{-3} NCC d^{-1}. There was very little color removal at 100 Ω, and the corresponding cathode potential was about −172 mV vs SHE.

The effect of cathodic HRT on AO7 decolorization was investigated in the range of 0.31−3.75 h, as shown in SI Figure S1(B). As cathodic HRT increased, the AO7 decolorization efficiency increased from 34.6 ± 1.8% to 90.0 ± 1.5%, demonstrating a positive relation between the cathodic HRT and color removal efficiency. The same trend was also obtained in anaerobic biological processes for color removal but with a longer HRT of 6−12 h (*25, 26*). On the contrary, the AO7 decolorization rate was decreased with prolonging HRT, from 5.05 ± 0.27 to 1.10 ± 0.02 mol m^{-3} NCC d^{-1} in BES.

The effect of the pH at the cathode on the AO7 decolorization process was examined, and the results are shown in SI Figure S1(C). Because the experiments performed at influent pH 5.5 and 9.4 had nearly no buffering capacity, the pH in the cathode chamber increased to 6.2 and 10.0 respectively. Protons are consumed in an equimolar ratio to electrons in the cathodic reaction at the cathode and consequently, in the absence of pH control the pH will increase in the cathode chamber if protons are not replenished through the membrane (*27*). The results in SI Figure S1(C) are presented according to the pH in the cathode chamber. The AO7 decolorization efficiency decreased from 90.4 ± 0.9% to 19.2 ± 0.9% with the increase of pH at the cathode from 6.2 to 10.0. Correspondingly, the AO7 decolorization rate decreased from 2.83 ± 0.03 to 0.60 ± 0.03 mol m^{-3} NCC d^{-1} in the reactor. The cathode potential increased from −303 ± 5 to −260 ± 3 mV vs SHE with decreasing the pH in the cathode chamber, while the anode potential remained about −295 mV vs SHE (pH kept at 7.0 at the anode). This resulted in an increase of cell voltage and current. Hence, the AO7 decolorization efficiency and rate increased as the

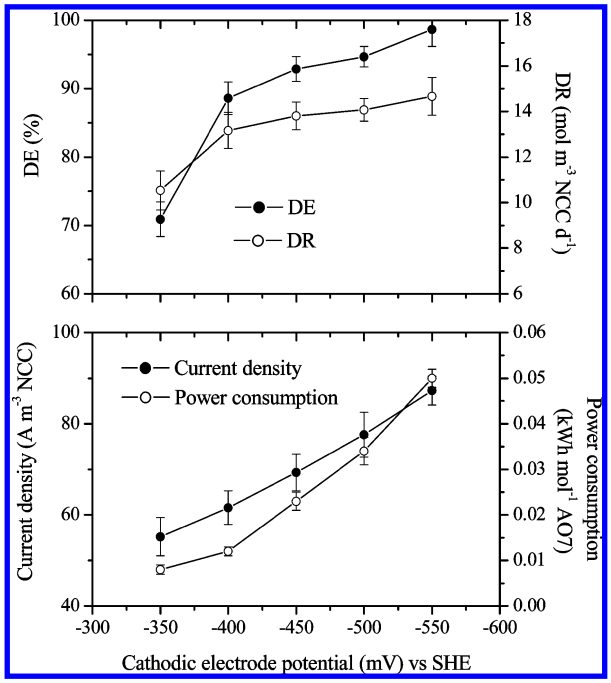

FIGURE 2. Effect of cathodic electrode potential on (A) decolorization efficiency (DE) and rate (DR), and (B) current density and power consumption in BES (influent AO7 concentration 0.89 mM, HRT 1.44 h).

reactor pH of cathode decreased. In addition, as the concentration of phosphate buffer in the influent AO7 solution was reduced from 50 mM to 0, the AO7 decolorization rate significantly decreased from 2.45 ± 0.02 to 0.28 ± 0.02 mol m^{-3} NCC d^{-1}. Without phosphate buffer in the influent AO7 solution, the pH in the cathode chamber was increased to 8.7. These results clearly indicate that it is very important to avoid pH increases at the cathode in order to maintain the high decolorization activity in BESs. While the addition of a phosphate buffer into the cathode of a BES is not economically feasible or environmentally sensible, most wastewaters have a reasonably good buffering capacity, mainly in the form of bicarbonate. Alternative ways have also been suggested in previous studies including the loop configuration of BESs (*24*) and addition of bicarbonate buffer generated from the self-produced CO_2 in BESs (*28*).

Enhancing AO7 Decolorization with Controlled Cathode Potential. The AO7 decolorization activities were significantly enhanced by controlling the cathodic electrode potential in the range of −350 to −550 mV vs SHE, as shown in Figure 2(A). Both the decolorization efficiency and rate of AO7 increased with a decreasing cathodic electrode potential. The AO7 decolorization efficiency increased from 70.9 ± 2.6% to 98.7 ± 2.5%, and correspondingly, the decolorization rate increased from 10.53 ± 0.85 to 14.66 ± 0.83 mol m^{-3} NCC d^{-1}. This result also clearly indicates that cathodic electrode potential has a drastic influence on the azo dye decolorization in the BES. A more negative cathode potential means a more reduced environment that may be more favorable to electron transfer from cathode to azo bond for decolorization.

Since the minimum open circuit potential of the bioanode is about −330 mV vs SHE using acetate as electron donor, additional voltage and hence power had to be supplied to the BES reactor in order to control the cathodic electrode potential to less than −350 mV vs SHE. Figure 2(B) shows the changes of the current density and power consumption as the cathodic electrode potential decreased form −350 mV vs SHE to −550 mV vs SHE. Both the current density and power consumption (from potentiostat) increased with the decrease of cathodic electrode potential, from 55.2 ± 4.2 to 87.3 ± 3.2 A m^{-3} NCC and 0.008 ± 0.001 to 0.05 ± 0.002 kWh mol^{-1} AO7, respectively. It is very interesting to note that the power consumption was drastically reduced compared to the pure electrochemical reduction method with a reported energy consumption of about 11.2 kWh mol^{-1} azo dye (*7*). First, the microbial oxidation of acetate at the anode provides a renewable source of energy for AO7 decolorization, and overall greatly reduces the energy needed. Second, the anode reaction is catalyzed by self-sustaining microbial biocatalysts, resulting in a significantly reduced overpotential.

Coulombic Efficiencies. The Coulombic efficiencies did not exceed 55% at the anodes of BES (Table 1). In Freguia et al. (*29*), bacterial growth was found to be the predominant cause for the decrease of the Coulombic efficiency at the anode during batch operations. Besides, other processes such as fermentation and methanogenesis may also compete for the utilization of the available substrate (*12*). In this study, the anodic potentials were low at any influent AO7 concentration applied (below −290 mV vs SHE). This provided the bacteria growing at the anodic electrode surface with very limited energy gain and may favor alternative processes. Acetoclastic methanogenesis and bacterial growth were speculated to both be causes for the low Coulombic efficiencies obtained at the anode (*20*). A detailed investigation of these processes in a very similar anode system has been undertaken previously by Freguia et al. (*29*). However, further investigations are necessary to better clarify the nature of these competitive anodic processes and minimize their occurrence.

The Coulombic efficiency of the AO7 reduction at the cathode was evaluated as the ratio of the current that would be obtained as a result of the complete breakdown of the AO7 azo bond and the current flowing across the BES. As shown in Table 1, the Coulombic efficiency for AO7 decolorization was higher than 77.4%, indicating that a majority of electrons from cathode electrode were used for AO7 decolorization, i.e., the azo bond breakdown at the cathode. However, the purity of AO7 dye used in this study was only 93% and hence some other electron acceptors might also be present. In addition, the SA concentration of cathode effluent was quantified using HPLC, and the results are shown in Table 1. The Coulombic efficiency for SA formation was estimated as the ratio of the theoretical current required based on the SA production from AO7 at the cathode and the actual current flowing across the BES. The values at various influent AO7 concentrations were higher than 80%, further demonstrating that most of the electrons from the cathode were used for the reduction of the azo-bond in AO7.

On the other hand, O_2 is the most plausible sink of electrons and can compete with the electrode at the anode and/or with AO7 at the cathode as electron acceptor, resulting in reduced Coulombic efficiencies at both compartments. However, various precautions have been taken in this study to avoid introducing O_2 into the BES, which seem to have been successful in previous studies with very similar reactor systems (*28*). Therefore, oxygen introduction is not expected to have a significant impact on the electron balance at both the anode and the cathode in this study.

The reductant usage ratio (RUR) as shown in Table 1 was also calculated at various influent AO7 concentrations according to eq 7. In theory, only one COD-mol acetate is needed for one mole of AO7 decolorization. However, the RURs varied from 2.2 ± 0.3 to 3.5 ± 0.2 mol COD mol^{-1} AO7 due to the electron inefficiencies at both the anode and the cathode.

Decolorization Mechanism. SI Figure S2 illustrates the UV−vis absorption spectra of the initial solutions and the decolorized samples for AO7 from the BES. There were three characteristic absorbance peaks at 228, 310, and 484 nm for AO7. The former two peaks derived from aromatic rings, and

TABLE 1. Coulombic Efficiency (CE) and Reductant Usage Ratio at Various Influent AO7 Concentrations in BES

influent AO7 (mM)	effluent AO7 (mM)	effluent SA (mM)	CE on AO7 decolorization (%)	CE on SA formation (%)	CE on acetate oxidation (%)	reductant usage ratio (mol COD mol^{-1} AO7)
0.19	0.040 ± 0.009	0.16 ± 0.01	77.4 ± 0.7	80.1 ± 0.1	36.8 ± 2.0	3.5 ± 0.2
0.40	0.182 ± 0.008	0.19 ± 0.01	89.2 ± 3.2	81.9 ± 0.1	44.2 ± 2.8	2.5 ± 0.2
0.59	0.355 ± 0.011	0.22 ± 0.01	92.6 ± 4.2	87.2 ± 0.1	44.5 ± 2.8	2.5 ± 0.3
0.70	0.457 ± 0.014	0.26 ± 0.01	92.2 ± 5.4	95.4 ± 0.1	49.5 ± 3.0	2.2 ± 0.3

the latter peak from the conjugated structure formed by the azo bond. After decolorization, the characteristic absorption peaks of AO7 were significantly decreased, while simultaneously a new peak appeared at 245 nm. These results demonstrate the cleavage of the azo bond and the formation of breakdown products at the cathode of BES. When AO7 was reduced, the azo double bond was destroyed, and the absorbance at 484 nm was almost completely removed.

The cathode effluent samples were analyzed by HPLC to further identify the reduced products of the AO7 decolorization. SI Figure S3 shows the HPLC chromatogram of the cathode influent and effluent. The main peaks in the effluent with retention times of 1.85 and 4.12 min match exactly the retention times of sulfanilic acid and 1-amino-2-naphthol respectively, indicating that these two compounds were the dominant products of the AO7 decolorization at the cathode. The smaller peaks in the effluent chromatogram might be related to oxidative products of 1-amino-2-naphthol, which has been reported to easily undergo autoxidation reactions even in the presence of only low amounts of oxygen in the solution (*30*).

Based on the degradation products identified and qualified, as well as the high Coulombic efficiency on AO7 decolorization and SA formation at the cathode, the possible decolorization mechanism of AO7 in BES systems is suggested in Figure 3. At the anode, acetate was oxidized by bacteria to produce protons and electrons, which were transferred to the cathode. At the cathode, the azo bond of AO7 was broken using proton and electron, resulting in the formation of colorless products of sulfanilic acid and 1-amino-2-naphthol. Since these breakdown products are also toxic (*22*), a second

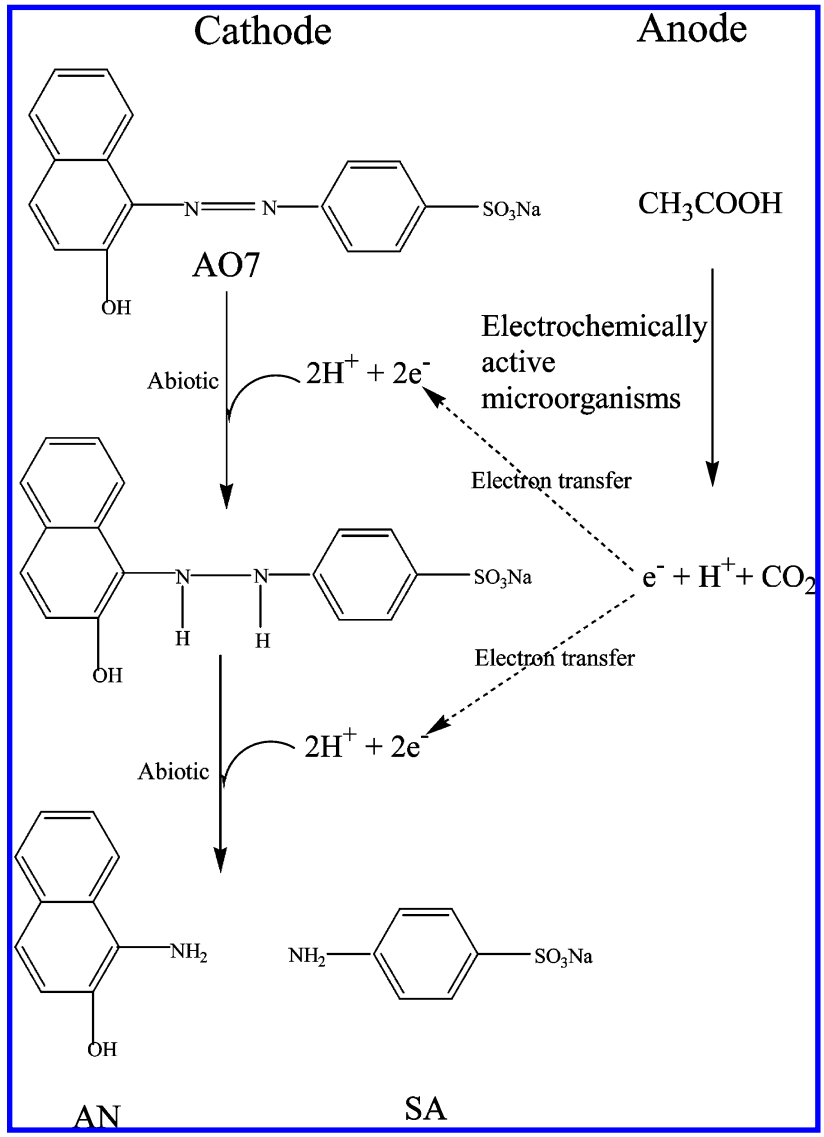

FIGURE 3. Possible AO7 decolorization mechanism in BES.

treatment process such as aerobic treatment is necessary to further degrade or mineralize these breakdown products.

Comparison with Anaerobic Biological Methods. SI Table S2 shows a summary of the AO7 decolorization through various biological methods for comparison. At a very short HRT (1.44 h) without power input, the cathodic decolorization rate of BES was comparable with other biological methods. However, this method could achieve possible energy recovery since current was generated spontaneously (no energy input) during this process.

To overcome the problem of slow azo dye reduction rate in the anaerobic biological processes, redox mediators like quinones are usually added to speed up reaction rates by shuttling reducing equivalents between (terminal) electron donors and electron acceptors (*31*). However, the addition of these redox mediators into the systems is not only unpractical particular in continuous reactors but also possibly toxic to the bacteria. In this study, the AO7 decolorization rate could be further enhanced by supplying some power to the BES systems (e.g., through cathodic potential control as shown in SI Table S2), which demonstrates that the decolorization of AO7 was highly effective at the cathode of BESs. For practical application purposes, a controlled potential of −400 mV vs SHE could be applied as this would increase the decolorization rate about 5-fold, while the reductant usage ratio was increased by only 40% and the power input is quite low at 0.012 kWh mol^{-1} AO7. For a typical dye bath wastewater with 100 mg/L of azo dye (assumed as AO7), the power required for the azo-bond reduction in a BES would be in the order of 0.04 kWh m^{-3} treated wastewater.

In the anaerobic biological decolorization removal methods, an electron donor (organic cosubstrate) is required to create the necessary reductive conditions. The decolorization rate of conventional anaerobic biological methods is very slow, and the cosubstrate addition typically far exceeds the stoichiometric requirements as shown by the high RUR values in SI Table S2. This creates considerable costs and leads to possibly unwanted methane formation (*11*). The RUR values for the BES are considerably smaller than those of anaerobic methods, indicating that very limited organic substrate is required for the bioelectrochemical decolorization of AO7. Furthermore, this substrate is provided in the anode compartment and can therefore primarily consist of wastewater organics from the dyeing operations, which are usually present in more than sufficient quantities.

The membrane biofilm reactor is a new technology using hydrogen as the electron donor for reduction of xenobiotics, such as trichloroethene, and *N*-nitrosodimethylamine (*32, 33*). In contrast to organic electron donors, hydrogen leaves no residuals. Similar to the organic electron donor used in this study, hydrogen is nontoxic and is relatively inexpensive. However, hydrogen has a low water solubility and a risk of forming a combustible atmosphere when mixed with air, which are two key considerations the membrane biofilm reactor aims to overcome. Unfortunately, a direct comparison with the performance of the BES is not feasible at this stage as to our knowledge no studies have been reported on azo dye decolorization using the H_2 membrane biofilm reactor.

Acknowledgments

We thank David Rosolen for his support with the HPLC analysis. This research was supported by the Australian Research Council (Grant DP0666927, DP0879245 and DP0985317) and the UQ Early Career Research Scheme (2007002078).

Supporting Information Available

Experimental setup for cathode in Table S1; Comparison of AO7 decolorization with anaerobic biological methods in Table S2; Effect of several key parameters on AO7 decolorization in Figure S1; UV−vis spectra and HPLC chromatogram for products identification in Figures S2 and S3 respectively. This material is available free of charge via the Internet at http://pubs.acs.org.

Literature Cited

(1) O'Neill, C.; Hawkes, F. R.; Hawkes, D. L.; Lourenco, N. D.; Pinheiro, H. M.; Delee, W. Colour in textile effluents sources, measurement, discharge consents and simulation: a review. *J. Chem. Technol. Biotechnol.* **1999**, *74*, 1009–1018.

(2) Ganesh, R.; Boardman, G. D.; Michelson, D. Fate of azo dyes in sludges. *Water Res.* **1994**, *28*, 1367–1376.

(3) Selvam, K.; Swaminathan, K.; Chae, K. S. Microbial decolourization of azo dyes and dye industry effluent by Fomes lividus. *World J. Microbiol. Biotechnol.* **2003**, *19*, 591–593.

(4) Mu, Y.; Yu, H. Q.; Zheng, J. C.; Zhang, S. J. TiO_2-mediated photocatalytic degradation of Orange II with the presence of Mn^{2+} in solution. *J. Photochem. Photobiol. A* **2004**, *163*, 311–316.

(5) Golab, V.; Vinder, A.; Simonic, M. Efficiency of the coagulation/flocculation method for the treatment of dye bath effluent. *Dyes Pigm.* **2005**, *67*, 93–97.

(6) Pandey, A.; Singh, P.; Iyengar, L. Bacterial decolourization and degradation of azo dyes. *Int. Biodeterior. Biodegrad.* **2007**, *59*, 73–84.

(7) Bechtold, T.; Burtscher, E.; Turcanu, A. Cathodic decolourisation of textile waste water containing reactive dyes using a multi-cathode eletrolyser. *J. Chem. Technol. Biotechnol.* **2001**, *76*, 303–311.

(8) Bechtold, T.; Turcanu, A. Cathodic decolourisation of dyes in concentrates from nanofiltration and printing pastes. *J. Appl. Electrochem.* **2004**, *34*, 903–910.

(9) Shaul, G. M.; Holdsworth, T. J.; Dempsey, C. R.; Dostal, K. A. Fate of water-soluble azo dyes in the activated-sludge process. *Chemosphere* **1991**, *22*, 107–119.

(10) dos Santos, A. B.; Traverse, J.; Cervantes, F. J.; van Lier, J. B. Enhancing the electron transfer capacity and subsequent colour removal in bioreactors by applying thermophilic anaerobic treatment and redox mediators. *Biotechnol. Bioeng.* **2005**, *89*, 42–52.

(11) van der Zee, F. P.; Villaverde, S. Combined anaerobic-aerobic treatment of azo dyes - A short review of bioreactor studies. *Water Res.* **2005**, *39*, 1425–1440.

(12) Logan, B. E.; Hamelers, B.; Rozendal, R.; Schrorder, U.; Keller, J.; Freguia, S.; Aelterman, P.; Verstraete, W.; Rabaey, K. Microbial fuel cells: Methodology and technology. *Environ. Sci. Technol.* **2006**, *40*, 5181–5192.

(13) Rozendal, R. A.; Hamelers, H. V. M.; Euverink, G. J. W.; Metz, S. J.; Buisman, C. J. N. Principle and perspectives of hydrogen production through biocatalyzed electrolysis. *Int. J. Hydrogen Energy* **2006**, *31*, 1632–1640.

(14) Rozendal, R. A.; Hamelers, H. V. M.; Rabaey, K.; Keller, J.; Buisman, C. J. N. Towards practical implementation of bioelectrochemical wastewater treatment. *Trends Biotechnol.* **2008**, *26*, 450–459.

(15) Liu, H.; Cheng, S. A.; Logan, B. E. Production of electricity from acetate or butyrate using a single-chamber microbial fuel cell. *Environ. Sci. Technol.* **2005**, *39*, 658–662.

(16) Ren, Z. Y.; Ward, T. E.; Regan, J. M. Electricity production from cellulose in a microbial fuel cell using a defined binary culture. *Environ. Sci. Technol.* **2007**, *41*, 4781–4786.

(17) de Schamphelaire, L.; van den Bossche, L.; Dang, H. S.; Hofte, M.; Boon, N.; Rabaey, K.; Verstraete, W. Microbial fuel cells generating electricity from rhizodeposits of rice plants. *Environ. Sci. Technol.* **2008**, *42*, 3053–3058.

(18) Rabaey, K.; Van de Sompel, K.; Maignien, L.; Boon, N.; Aelterman, P.; Clauwaert, P.; De Schamphelaire, L.; Pham, H. T.; Vermeulen, J.; Verhaege, M.; Lens, P.; Verstraete, W. Microbial fuel cells for sulfide removal. *Environ. Sci. Technol.* **2006**, *40*, 5218–5224.

(19) Clauwaert, P.; Rabaey, K.; Aelterman, P.; Schamphelaire, L. D.; Pham, T. H.; Boeckx, P.; Boon, N.; Verstraete, W. Biological denitrification in microbial fuel cells. *Environ. Sci. Technol.* **2007**, *41*, 3354–3360.

(20) Virdis, B.; Rabaey, K.; Yuan, Z. G.; Keller, J. Microbial fuel cells for simultaneous carbon and nitrogen removal. *Water Res.* **2008**, *42*, 3013–3024.

(21) Aulenta, F.; Catervi, A.; Majone, M.; Panero, S.; Reale, P.; Rossetti, S. Electron transfer from a solid-state electrode assisted by methyl viologen sustains efficient microbial

reductive dechlorination of TCE. *Environ. Sci. Technol.* **2007**, *41*, 2554–2559.
(22) van der Zee, F. P.; Bisschops, I. A. E.; Lettinga, G. Activated carbon as an electron acceptor and redox mediator during the anaerobic biotransformation of azo dyes. *Environ. Sci. Technol.* **2003**, *37*, 402–408.
(23) Freguia, S.; Rabaey, K.; Yuan, Z. G.; Keller, J. Sequential anode-cathode configuration improves cathodic oxygen reduction and effluent quality of microbial fuel cells. *Water Res.* **2008**, *42*, 1387–1396.
(24) Rabaey, K.; Ossieur, W.; Verhaege, M.; Verstraete, W. Continuous microbial fuel cells convert carbohydrates to electricity. *Water Sci. Technol.* **2005**, *52*, 515–523.
(25) Kapdan, I. K.; Tekol, M.; Sengul, F. Decolourization of simulated textile wastewater in an anaerobic-aerobic sequential treatment system. *Process Biochem.* **2003**, *38*, 1031–1037.
(26) Albuquerque, M. G. E.; Lopes, A. T.; Serralheiro, M. L.; Novais, J. M.; Pinheiro, H. M. Biological sulphate reduction and redox mediator effects on azo dye decolourisation in anaerobic-aerobic sequencing batch reactors. *Enzyme Microb. Technol.* **2005**, *36*, 790–799.
(27) Rozendal, R. A.; Hamelers, H. M.; Buisman, C. N. Effects of membrane cation transport on pH and microbial fuel cell performance. *Environ. Sci. Technol.* **2006**, *40*, 5206–5211.
(28) Fan, Y. Z.; Hu, H. Q.; Liu, H. Sustainable power generation in microbial fuel cells using bicarbonate buffer and proton transfer mechanisms. *Environ. Sci. Technol.* **2007**, *41*, 8154–8158.
(29) Freguia, S.; Rabaey, K.; Yuan, Z.; Keller, J. Electron and carbon balances in microbial fuel cells reveal temporary bacterial storage behaviour during electricity generation. *Environ. Sci. Technol.* **2007**, *41*, 2915–2921.
(30) Kudlich, M.; Hetheridge, M. J.; Knackmuss, H. J.; Stolz, A. Autoxidation reactions of different aromatic o-Aminohydroxy-naphthalenes that are formed during the anaerobic reduction of sulfonated azo dyes. *Environ. Sci. Technol.* **1999**, *33*, 896–901.
(31) van der Zee, F. P.; Bouwman, R. H. M.; Strik, D. P. B. T. B.; Lettinga, G.; Field, J. A. Application of redox mediators to accelerate the transformation of reactive azo dyes in anaerobic bioreactors. *Biotechnol. Bioeng.* **2001**, *75*, 691–701.
(32) Chung, J.; Krajmalnik-Brown, R.; Rittmann, B. E. Bioreduction of trichloroethene using a hydrogen-based membrane biofilm reactor. *Environ. Sci. Technol.* **2008**, *42*, 477–483.
(33) Chung, J.; Ahn, C. H.; Chen, Z.; Rittmann, B. E. Bio-reduction of *N*-nitrosodimethylamine (NDMA) using a hydrogen-based membrane biofilm reactor. *Chemosphere* **2008**, *70*, 516–520.

ES900057F